Published by Associazione Teriologica Italiana
Hystrix, the Italian Journal of Mammalogy
Volume 24 (1): 33–41, 2013
Available online at:
http://www.italian-journal-of-mammalogy.it/article/view/6383/pdf
doi:10.4404/hystrix-24.1-6383

Research Article

Phylogenetic Principal Components Analysis and Geometric Morphometrics

P. David Polly[a,*], A. Michelle Lawing[b], Anne-Claire Fabre[c,d], Anjali Goswami[c]

[a] *Departments of Geological Sciences, Biology, and Anthropology, Indiana University, 1001 E. 10th Street, Bloomington, IN 47405, USA*
[b] *Departments of Geological Sciences and Biology, Indiana University, 1001 E. 10th Street, Bloomington, IN 47405, USA*
[c] *Departments of Genetics, Evolution & Environment and Earth Sciences, University College London, Gower Street, London WC1E 6BT, UK*
[d] *Muséum National d'Histoire Naturelle, UMR 7207 - Centre de Recherche sur la Paléobiodiversité & les Paléoenvironnements, 8 rue Buffon - CP 38, F-75231 Paris cedex 05, France*

Keywords:
phylogenetic principal component analysis
geometric morphometrics
comparative phylogenetic methods
shape analysis

Article history:
Received: 28 July 2012
Accepted: 19 September 2012

Acknowledgements
The authors thank Andrea Cardini and Anna Loy for inviting them to contribute to this volume. Leandro Monteiro, Andrea Cardini, and an anonymous reviewer made suggestions that helped improve the manuscript. Jim Rohlf, Joe Felsenstein, and Emilia Martins discussed some of the equations that were used in the Mathematica code used to perform many of the analyses presented in this paper. We thank Jacques Cuisin, Géraldine Véron and Julie Villemain for access to specimens from the Laboratoire Mammifères et Oiseaux, MNHN, Paris, and Loïc Costeur for the loan of material from the Naturhistorisches Museum, Basel. Raphael Cornette and Stéphane Peigné provided extensive help and support during data collection and template construction for the humerus datsaset. A-CF would like to thank the UMS CNRS/MNHN 2700, "Outils et Méthodes de la Systématique Intégrative",for access to the Plate-forme de Morphométrie and the Ecole doctorale interdisciplinaire Européene Frontières du vivant ED474 program doctoral Liliane Bettencourt for support during data collection. Mathematica code to perform most of the analyses presented here is available at http://mypage.iu.edu/~pdpolly/Software.html.

Abstract

Phylogenetic Principal Components Analysis (pPCA) is a recently proposed method for ordinating multivariate data in a way that takes into account the phylogenetic non-independence among species means. We review this method in terms of geometric morphometric shape analysis and compare its properties to ordinary principal components analysis (PCA). We find that pPCA produces a shape space that preserves the Procrustes distances between objects, that allows shape models to be constructed, and that produces scores that can be used as shape variables for most purposes. Unlike ordinary PCA scores, however, the scores on pPC axes are correlated with one another and their variances do not correspond to the eigenvalues of the phylogenetically corrected axes. The pPC axes are oriented by the non-phylogenetic component of shape variation, but the positioning of the scores in the space retains phylogenetic covariance making the visual information presented in plots a hybrid of non-phylogenetic and phylogenetic. Presuming that all pPCA scores are used as shape variables, there is no difference between them and PCA scores for the construction of distance-based trees (such as UPGMA), for morphological disparity, or for ordinary multivariate statistical analyses (so long as the algorithms are suitable for correlated variables). pPCA scores yield different trait-based trees (such as maximum likelihood trees for continuous traits) because the scores are correlated and because the pPC axes differ from PC axes. pPCA eigenvalues represent the residual shape variance once the phylogenetic covariance has been removed (though there are scaling issues), and as such they provide information on covariance that is independent of phylogeny. Tests for modularity on pPCA eigenvalues will therefore yield different results than ordinary PCA eigenvalues. pPCA can be considered another tool in the kit of geometric morphometrics, but one whose properties are more difficult to interpret than ordinary PCA.

Introduction

Principal Component Analysis (PCA) is an important step in geometric morphometrics, both in its own right as a tool to understand overall patterns of shape variation and as a means for producing mathematically uncorrelated shape variables to use in subsequent analyses (Bookstein, 1997a; Dryden and Mardia, 1998). Even though PCA shape variables are mathematically uncorrelated, they may be phylogenetically correlated when shape is sampled in populations or species that are phylogenetically structured. Techniques for analyzing phylogenetically structured data exist, such as mapping shape data onto phylogenies or removing phylogenetic correlations from data, but confusion remains about what these techniques do and when they should be applied. The confusion is compounded by the term "phylogenetic comparative methods", which is applied both to techniques that highlight phylogenetic changes and techniques that remove the effects of phylogeny. Studies of evolution, adaptation, and systematics benefit from techniques that incorporate phylogeny, while studies of correlations that originate from physical processes or other non-adaptive factors benefit from techniques that remove phylogeny.

Phylogenetic principal components analysis (pPCA) is a method recently proposed for controlling for phylogenetic covariance to produce a PCA-like ordination (Revell, 2009). The major axes of pPCA shape space are not the major axes of shape variation, as in ordinary PCA, but rather the major axes of the non-phylogenetic residual variation once phylogenetic covariation has been removed. Note that pPCA is an ordination that attempts to correct for shared phylogenetic history in constructing the axes, which is very different from methods that simply project phylogenetic trees into morphospace and which are referred to by some as "phylogenetic principal components analysis" (e.g., Rohlf 2002; Polly 2008; Klingenberg and Gidaszewski 2010). pPCA can ostensibly be used to study shape variation that arises from underlying processes that are common to all taxa, such as allometric scaling in quadrupedal animals between body mass and limb structure. Because pPCA has rapidly gained popularity in evolutionary studies (e.g., Bergmann and Berk 2012; Kohlsdorf and Navas 2012), we feel it is timely to review its properties in the context of geometric morphometrics. As anticipated by Revell (2009), we find that phylogenetic correlation is not removed by pPCA, and we also find the pPCA scores are correlated between axes and that the variance of scores on pPC axes does not necessarily decrease with sequentially higher axes.

To demonstrate these findings, we critically compare pPCA with ordinary PCA in the context of geometric morphometrics. As a preface, we review PCA, including the essential properties of eigenvectors, eigenvalues, and scores, to provide a clear point of comparison for how pPCA differs. We show with simulated and real examples that pPCA scores have several underappreciated properties, most importantly that they are a rigid rotation of PCA scores and thus conserve between-

*Corresponding author
Email address: pdpolly@indiana.edu (P. David Polly)

specimen distances when measured in the full multivariate space and that the scores on different pPCA axes can be highly correlated with one another. We evaluate how these properties impact some of the standard multivariate analyses used in geometric morphometrics.

A review of principal components analysis

Before discussing pPCA, it is useful to review the technical properties and uses of ordinary PCA in geometric morphometrics. PCA is an ordination technique that is frequently used in multivariate morphometrics. In geometric morphometrics, PCA is one of two preferred methods for producing shape variables that are uncorrelated with one another and whose dimensionality is appropriate for further statistical analysis, the other method being partial warps analysis (Rohlf, 1993; Dryden and Mardia, 1998; Zelditch et al., 2004). Relative Warps Analysis (Rohlf, 1993) is a PCA of partial warp scores and is identical to ordinary shape PCA when the uniform component of shape is included and when the principal warps are weighted equally. PCA space is therefore the standard "shape space" used to show similarity and difference in shape among objects, and it is often used to model evolutionary and developmental shape transformations (e.g., Mitteroecker et al. 2004; Polly 2004; Adams and Collyer 2009). Principal component axes (PCs) function as shape variables, the first of which represents the major axis of variation among the objects. Successive PCs are orthogonal, or at right angles, to the first PC and to each other along the successively greatest axes of variation among the objects. Because the first two or three axes often represent most of the variation in the data set, plots of objects on these axes show most of the overall similarity and difference in shape. Many variations of PCA exist, and readers are referred to Jollife (2002) for a comprehensive description. Here we discuss properties of the simplest form of PCA where the ordination of objects is mean centered and based on the covariance matrix of the variables. The features of PCA that are most relevant to our discussion are the covariance matrix ($\mathbf{P}$), the eigenvectors ($\mathbf{U}$) and eigenvalues ($\mathbf{\Sigma}$) of $\mathbf{P}$, and the scores ($\mathbf{S}$) of the objects on the eigenvectors.

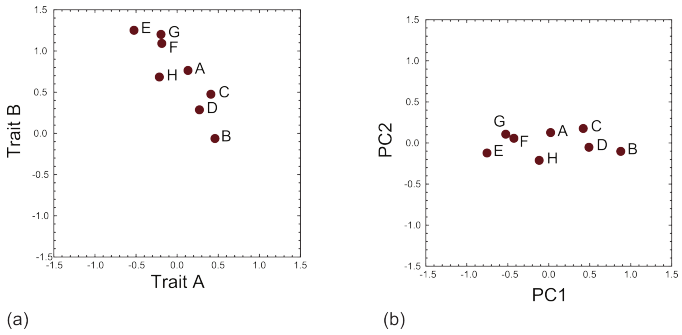

Figure 1 – Example showing the conservation of variance in PCA using a covariance matrix. (a) Data plotted in trait space, where the two clades are separated by both traits. (b) Data plotted in principal components space, where PC 1 separates the two clades. Note that for two traits, there are only two principal components so no other dimensions exist in the trait or PC spaces than those shown.

$\mathbf{P}$ is a symmetrical $m \times m$ matrix of the covariances between the m traits in the off-diagonal elements and the variances in the diagonal elements. In geometric morphometrics, the traits that go into this matrix are the mean-centered landmark coordinates of the objects after Procrustes superimposition. The trace of $\mathbf{P}$, which is the sum of its diagonal elements, is self-evidently equal to the sum of the variances of each of the superimposed landmark coordinates. For later reference, note that $\mathbf{P}$ is calculated as:

$$\mathbf{P} = (n-1)^{-1}(\mathbf{X} - mean[\mathbf{X}])^{\top} \cdot (\mathbf{X} - mean[\mathbf{X}]) \qquad (1)$$

where n is the number of taxa and $\mathbf{X}$ is a matrix of trait values. Note that the rank of this matrix is less than m, the number of traits, because $\mathbf{X}$ is a matrix of Procrustes superimposed coordinates where size, translation, and rotation have been removed, thus removing four degrees of freedom from two-dimensional landmark data $(2m-4)$ and seven for three-dimensional data $(3m-7)$ Rohlf and Slice (1990); Bookstein (1997a). The Procrustes coordinates are thus said to be "collinear" and $\mathbf{P}$ is said to be "singular" because of the loss of these degrees of freedom. The Procrustes coordinates are thus non-independent, violating the assumptions of many statistical analyses. The relevance to PCA is that the loss of degrees of freedom results in fewer PC axes than there are landmark coordinates and that PCA scores provide uncorrelated shape variables that can be used in place of the correlated Procrustes coordinates.

PC axes are defined by the eigenvectors of $\mathbf{P}$ and the variance of the objects on each of the axes is given by the eigenvalues. The term "objects" refers to the individual specimens or taxa that are being analyzed or, more technically, the variables used to measure the objects. In geometric morphometrics, the objects are represented by constellations of Procrustes superimposed points. The elements of the eigenvectors are the cosines of the angles (in radians) of each vector from each of the original variables (the Procrustes residuals in the case of geometric morphometrics). Because $\mathbf{P}$ is singular, $\mathbf{U}$ and $\mathbf{\Sigma}$ are usually calculated using the singular-value decomposition algorithm (SVD) where $\mathbf{P} = \mathbf{U} \cdot \mathbf{\Sigma} \cdot \mathbf{V}^{\top}$ (e.g., Dryden and Mardia 1998). In some implementations of SVD the matrix $\mathbf{\Sigma}$ is a diagonal matrix of singular values, which are the square-roots of the eigenvalues, whereas in others $\mathbf{\Sigma}$ is returned as the eigenvalues themselves (our notation follows the latter). The scores, $\mathbf{S}$, are the values of the objects on the PC axes, or their coordinates in shape space. $\mathbf{S}$ is calculated by projecting the Procrustes residuals into the principal component space by multiplying the Procrustes residuals by the eigenvectors:

$$\mathbf{S} = (\mathbf{X} - mean[\mathbf{X}]) \cdot \mathbf{U} \qquad (2)$$

where $\mathbf{X}$ is the matrix of the Procrustes superimposed coordinates, $mean[\mathbf{X}]$ is the consensus shape or mean of the Procrustes coordinates. Because $\mathbf{U}$ contains the cosines of the angles between the original coordinates and the eigenvectors, Equation 2 describes the translation of the original data to the mean and rotation to its major axes of variation. Importantly for our later discussion, the eigenvectors can be thought of as describing the orientation of the objects in PC space and the eigenvalues can be thought of as their scaling in that space.

For the geometry of shape to be preserved in the PCA shape space, the variance and proportionality of the x, y, and z landmark coordinates must be maintained, as must the distances between the objects in the space (Rohlf, 1993; Dryden and Mardia, 1998). PCA based on a covariance matrix has such properties: the variances of the scores on the PC axes equal the corresponding eigenvalues, and so the sum of the variances of the scores equals the sum of the eigenvalues. Furthermore, because the scores are the result of a rigid rotation, the total variance of the original data set is preserved in the scores. In other words, the sum of the variances of the scores equals not only the sum of the eigenvalues, but also the sum of the variances of the original Procrustes coordinates and the sum of the diagonal of $\mathbf{P}$. Recall that a variance is the sum of squared deviations of objects from their mean divided by the number of objects. A Euclidean distance is the square root of the sum of squared differences of one object to another. The conservation of variance in PCA therefore also conserves the distances between objects in shape space.

Table 1 – Comparison of variances in original traits with the diagonal elements in their covariance matrix ($\mathbf{P}$), the eigenvalues of $\mathbf{P}$, and the variance of the PCA scores based on $\mathbf{P}$. The original trait variances and distances are preserved when the PCA is based on the covariance matrix. Fig. 1 shows ordinations associated with these data.

Variance of traits	
Trait A	0.123
Trait B	0.217
Total	0.340

Eigenvalues of $\mathbf{P}$	
Eigenvalue 1	0.320
Eigenvalue 2	0.020
Total	0.340

Trace of $\mathbf{P}$	
Trait A	0.123
Trait B	0.217
Total	0.340

Variance scores of $\mathbf{P}$	
PC 1	0.320
PC 2	0.020
Total	0.340

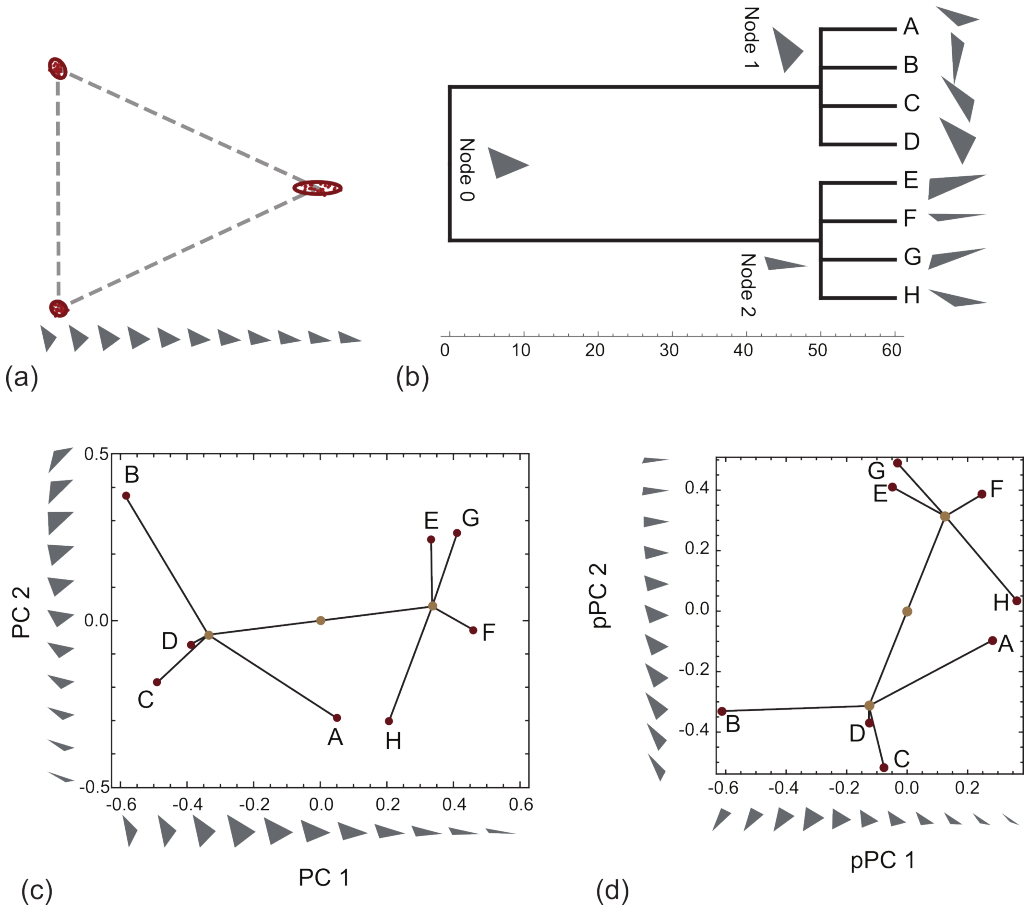

Figure 2 – A comparison of standard PCA and phylogenetic PCA using simulated evolution of eight triangles. (a) The apices of the triangles were simulated with covariances shown here. The grey triangles show the shape variation along the first eigenvector of the corresponding covariance matrix. (b) Triangles were simulated on the tree shown here using Brownian motion and the covariance matrix derived from a. After generating the eight tip shapes (shown in grey), ancestral node shapes were reconstructed on the tree (also shown in grey). (c) Ordinary PCA of the eight tip taxa from b. The phylogenetic tree has been projected into the PC space by locating the points in the space that correspond to the reconstructed ancestral node shapes. The shape variation described by each PC axis is shown as a series of small grey triangles along the two margins. (d) Phylogenetic PCA of the same data using the same conventions as in c. Note that shape space for triangles has only two dimensions ($2K - 4 = 6 - 4 = 2$) so the axes shown in c and d are the full shape space.

The example in Fig. 1 demonstrates the conservation of variance and inter-specimen distances in PCA. Randomly generated bivariate data for eight objects are plotted in trait space in Fig. 1a and in principal components space in Fig. 1b. One can see that the distances between the objects are preserved in the PC space, having been translated and rotated relative to the trait space. One can also see that in the PC space the objects are oriented along their major axis of variation. The sum of the variances of Traits A and B is the total variance in the data set, which is preserved in the sum of the variance of the scores on PC 1 and PC 2 and in the eigenvalues (Tab. 1). The mean distance between objects in the original trait space and in PC space is 0.730 units in both cases. Note that the PC space is mean centered and trait space is not.

Phylogenetic structure impacts PCA ordination, which is easily seen in the simulated example in Fig. 2. We simulated the evolution of triangles on a phylogenetic tree consisting of eight tip taxa in two distantly separated clades. We used triangles in this example because, after Procrustes superimposition, which removes 4 degrees of freedom for scaling, translation, and rotation, the shape space for triangles has only two dimensions allowing the full morphospace to be represented by just two principal components (Rohlf, 1999). We evolved the triangles on the tree (Fig. 2b) using Brownian motion and an arbitrarily defined population covariance (Fig. 2a). The major axis of this "generating" covariance is shown as a series of grey triangles in Fig. 2a. The eight simulated triangles and ancestral shapes reconstructed from them using a Brownian motion model (Martins and Hansen, 1997; Rohlf, 2001) are shown in Fig. 2b. The principal components of the triangles are shown in Fig. 2c, with the tree projected into the resulting shape space based on the node reconstructions (Rohlf, 2002; Polly, 2008). The shape variation described by each of the two PCs is shown as a series of grey triangles along the margins of the plot. The two clades form separate clusters in the plot, separated along PC 1, which is unsurprising because the branches separating the two clades are long and the greatest evolutionary differences are expected to accumulate along the longest branches. In fact, it is typical with data containing two or more clades that the first PC separates one group from the rest, the second PC separates another group, the third PC yet another, and etc. (in cases where there are more than two groups and two PCs). Also unsurprisingly, the shape variation associated with the first PC is similar to the generating covariance because the evolution along the two long branches separating the clades was simulated using that covariance structure. The structure of PC 1 is thus highly phylogenetic, but the shape variation along the axis is closely related to the underlying covariance used to simulate the data.

The code used to simulate these data, to perform the ancestral reconstructions, and to project the tree into shape space, as well as a complete description of the algorithms used, is available in the Geometric Morphometrics for Mathematica (v. 9.0) and the Phylogenetics for Mathematica (v. 2.1) packages (Polly, 2012a,b).

Properties of phylogenetic principal components analysis

Phylogenetic principal components analysis (pPCA) is similar to PCA, except that the covariance matrix is inversely weighted by phylogeny and the space is centered on the estimated phenotype of the root node of the tree instead of the mean of the tips (Revell, 2009). A key component of pPCA is the phylogenetic covariance matrix ($\mathbf{C}$), which is a symmetrical $n \times n$ matrix, where n is the number of tips on the tree, with off-diagonal elements containing the branch length shared by taxa and the diagonal elements containing the total branch length between

each tip and the root of the tree (Martins and Hansen, 1997; Rohlf, 2001; Revell, 2009). Under a Brownian motion model of evolution, this matrix describes the expected phenotypic variance and covariance among tip taxa due to common descent (Martins and Hansen, 1997; Felsenstein, 2003). Branch lengths can be given in any units, but, as elaborated below, the choice of units affects the eigenvalues of $\mathbf{C}$. In terms of geometric morphometrics, $\mathbf{C}$ describes the expected similarity in shape due to recency of common ancestry.

Following Revell (2009), the first step in pPCA is to estimate the ancestral node values of the traits on the tree:

$$a = [(\mathbf{1}^\top \cdot \mathbf{C}^{-1} \cdot \mathbf{1})^{-1} \cdot \mathbf{1}^\top \cdot \mathbf{C}^{-1} \cdot \mathbf{X}]^\top \quad (3)$$

which gives a vector of estimated ancestral values for the n traits ($\mathbf{X}$) at the root node of the tree, where $\mathbf{1}$ is a vector of ones whose length is equal to $\mathbf{C}$ and $\mathbf{X}$ is a matrix of Procrustes superimposed coordinates. This method for estimating ancestral node values is the same as the generalized linear model method (Martins and Hansen, 1997; Rohlf, 2001), and the ancestral node estimates are identical to maximum likelihood (Schluter et al., 1997) and squared-change parsimony (Maddison, 1991) estimates when the traits have evolved under a Brownian motion model. As Revell pointed out, methods that make different assumptions about evolution can be used in pPCA if so desired. The root node reconstruction is used to center the pPCA. Rohlf (1998) warned of distortions that could arise from the non-Euclidean curvature of shape space when values other than the arithmetic mean are used to center ordinations. In practice, the risk of such distortion is minimal because shape variation in biological data sets is usually small (Rohlf, 2003) and because the ancestral node reconstruction is merely a weighted mean and not radically different from the arithmetic mean, so we will not consider this issue further.

The next step in pPCA is to estimate the evolutionary covariance matrix for the traits ($\mathbf{P_P}$) (Revell, 2009). This matrix is similar to the ordinary trait covariance matrix ($\mathbf{P}$) except that taxa are weighted by their shared ancestry and traits are centered on the ancestral node values instead of their mean:

$$\mathbf{P_P} = (n-1)^{-1} \cdot (\mathbf{X} - a^\top)^\top \cdot \mathbf{C}^{-1} \cdot (\mathbf{X} - a^\top) \quad (4)$$

where n is the sample size and 1 is a scalar. Note that the calculation of $\mathbf{P_P}$ is identical to the calculation of $\mathbf{P}$ (Equation 1) except that the root ancestor is substituted for the mean and the inverse of $\mathbf{C}$ is used to weight the calculation. Because the elements of $\mathbf{C}$ are shared branch lengths, those taxa that share the longest branch lengths have the highest phylogenetic covariances are down-weighted most heavily by $\mathbf{C}$'s inverse. As with PCA, eigenvalues ($\mathbf{\Sigma_P}$) and eigenvectors ($\mathbf{U_P}$) are extracted from $\mathbf{P_P}$ using singular value decomposition. Note neither the sum of the diagonal elements of $\mathbf{P_P}$ nor the sum of its eigenvalues equal the sum of the variances in the original traits because of the weighting by the inverse of $\mathbf{C}$.

The final step of pPCA is to project the tip taxa into the space defined by the eigenvectors of $\mathbf{P_P}$ (Revell, 2009). The pPCA scores are calculated as

$$\mathbf{S_P} = (\mathbf{X} - a) \cdot \mathbf{U_P}. \quad (5)$$

Note the similarity and difference between Equations 2 and 5. Instead of being mean centered as in Equation 2, the traits $\mathbf{X}$ are centered on the root node a, and instead of being rotated to the eigenvectors of the covariance matrix $\mathbf{P}$ they are rotated to the eigenvectors of the phylogenetically weighted covariance matrix $\mathbf{P_P}$. Equation 5 is thus a rigid rotation of $\mathbf{X}$ around a just as Equation 2 is a rigid rotation of $\mathbf{X}$ around $mean[\mathbf{X}]$. The phylogenetic scores $\mathbf{S_P}$ are not rescaled by the eigenvalues $\mathbf{\Sigma_P}$, nor can they be without also changing their relative positions within the shape space. Revell (2009) rightly notes that the projection of the tip data $\mathbf{X}$ into the space defined by the eigenvectors makes pPCA different than an ordinary PCA of phylogenetically independent contrasts (Ackerly and Donoghue, 1998). The goal of pPCA is to ordinate the n tips rather than the $n-1$ contrasts, even though the goal of both is to provide a phylogenetically corrected ordination.

The PCA and pPCA ordinations are compared in Fig. 22c-d using the simulated triangle data set. In this example the two ordinations are visibly different (indeed, these particular simulated data were used because of their especially strong difference). One difference is the orientation of the objects within the space. PC 1 separates the two clades in the PCA plot because the greatest axis of phenotypic variation runs between the clades, but pPC 1 does not substantially separate the two groups because of the inverse weighting of $\mathbf{C}$ reduces the influence of shared differences of taxa, an effect that is most pronounced in the longest branches. Note, however, that clades 1 and 2 are just as distinct in the pPCA as in the PCA because the shape data themselves are not adjusted before projecting them onto the pPCA axes. All of the shape variation is therefore represented in pPCA because the calculation of scores is a rigid rotation of the original, ensuring that all the shape information is retained in both analyses. The plots differ, minorly, in where their axes are centered. In PCA the center of the axes is at the arithmetic mean of the tips (which happens to coincidentally be near Node 0 in this example), but in pPCA the center is precisely at the position of the basal node of the tree. The code for doing the pPCA ordination and projecting the phylogenetic tree into it is available in the Geometric Morphometrics for Mathematica package (version 9.0) (Polly, 2012a).

Table 2 – Trait variances in pPCA are not conserved. The sum of the variances of the tip traits does not equal the variances in the evolutionary covariance matrix $\mathbf{P_P}$ because of the adjustment for phylogenetic relationships. The sum of the variances of the pPCA axes, the eigenvalues, equals the variance in $\mathbf{P_P}$ but not the variance of the original traits. When the tips are projected into the pPCA space the sum of their variances is equal to the variance in the original data, but not the sum of the pPCA eigenvalues. Note that the variance of the scores on pPC 2 is greater their variance on pPC 1. The data summarized here are shown in Fig. 2.

Variance of Procrustes coordinates	
Apex 1x	0.055
Apex 1y	0.049
Apex 2x	0.016
Apex 2y	0.055
Apex 3x	0.047
Apex 3y	0.029
Total	0.251

Eigenvalues of $\mathbf{P}$	
Eigenvalue 1	0.182
Eigenvalue 2	0.069
Total	0.251

Eigenvalues of $\mathbf{P_P}$	
Eigenvalue 1	0.008
Eigenvalue 2	0.004
Total	0.011

Variance of scores of $\mathbf{P}$	
PC 1	0.182
PC 2	0.069
Total	0.251

Variance of scores of $\mathbf{P_P}$	
pPC 1	0.096
pPC 2	0.155
Total	0.251

An important property of pPCA is that, even though the pPC axes are orthogonal and they are numbered in descending order of their eigenvalues, the shape scores on the pPC axes are correlated and the proportion of the shape variance explained by them is not in descending order. In this example, the correlation between the pPC 1 and pPC 2 scores is 0.39 and the variance of the scores on pPC 2 is greater than on pPC 1 (Tab. 2). These unusual properties arise from the fact that phylogenetically adjusted trait data are used to construct the pPCA eigenvectors but unadjusted trait data are projected into them. We discuss these issues in detail in the following sections.

pPCA produces phylogenetically corrected eigenvalues and eigenvectors

The phylogenetic correction in pPCA adjusts the covariance matrix to remove the expected phylogenetic correlation among the traits (Revell, 2009), which it does very well. The effect of this adjustment is as though the tip data were adjusted to be no more divergent or correlated than if they had been drawn from a star phylogeny. The eigenvectors and eigenvalues of pPC 1 thus the major axis of non-phylogenetic variation, pPC 2 is the orthogonal major axis to the residual non-phylogenetic variation, and so on. The more phylogenetic structure there is among the tips, the more PCA and pPCA will differ. If the tips are drawn from a star phylogeny, the two ordinations will be

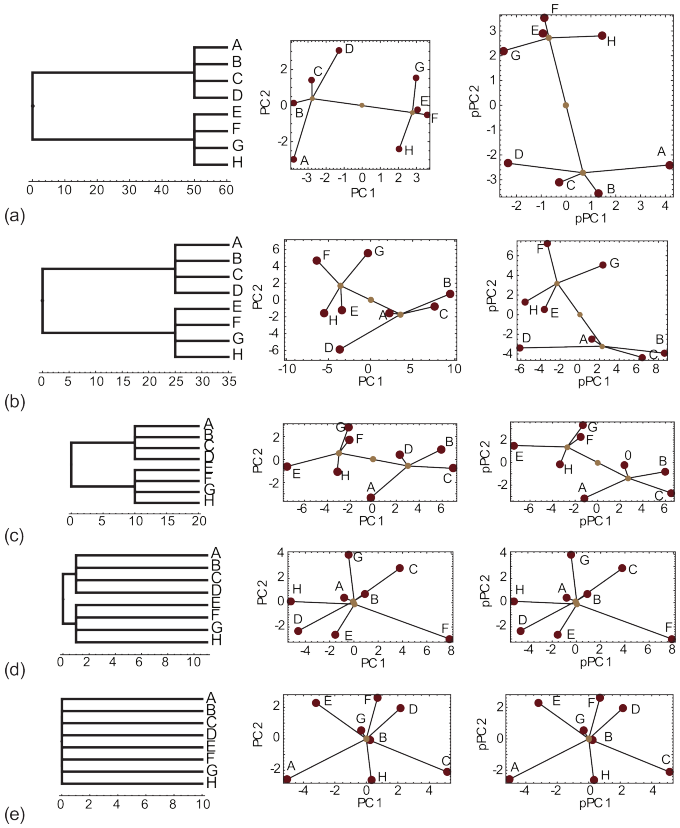

Figure 3 – Results of five simulations showing how phylogenetic structure affects PCA and pPCA ordinations. The evolution of two traits were simulated on the trees in the left column using a Brownian motion model. The PCA ordination of each simulated data set is shown in the center column and the pPCA ordination in the right column. When clades are separated by long branches (a) then the clades tend to be more different than their members and PC 1 tends to separate groups. pPCA adjusts for the phylogenetic separation and so pPC 1 differs substantially from PC 1. When the clades have shorter branches separating them than they have between members of a clade, then the between group differences tend to be small (b-d) and PC 1 is driven by non-phylogenetic variation and so does not differ substantially from pPC 1. As the tree topology approaches a star phylogeny (b-d) the PCA and pPCA ordinations become identical.

identical; and the farther the phylogeny is from a star, the more the two ordinations will differ (Fig. 3).

Note that the magnitudes of the pPCA eigenvalues depend on the units used for branch lengths and thus cannot be viewed as a simple proportion of the original shape variance. In our example, the sum of the eigenvalues is 0.011, but if the branch lengths are multiplied by 10 (e.g., if they were scaled in hundreds of thousands of years instead of millions of years) the sum of the eigenvalues declines to 0.001. In order for the pPCA eigenvalues to be proportional to the original shape variance, the branch lengths would have to be converted to phenotypic variance units so they would be on the same scale as the data (Rohlf, 2001; Felsenstein, 2003). In practice, the branch length units do not affect the pPCA ordination because the scale does not affect the orientation of the eigenvectors and the scores are not rescaled to have the same variance as the eigenvalues.

The variance of scores in pPCA space do not equal the eigenvalues of the pPCA vectors

Note that neither the eigenvalues ($\mathbf{\Sigma_P}$) nor the evolutionary covariance matrix ($\mathbf{P_P}$) are used to produce the scores (Equation 5); only the eigenvectors of $\mathbf{P_P}$ have an actual effect on the ordination. The eigenvectors describe the direction of the pPCA axes, and thus the orientation of the data, but not their variance or scale. pPCA thus affects only the orientation of the tips in the shape space, it does not change their overall variance or the distances among them, which is why Revell (2009) cautioned that subsequent statistical analyses still require phylogenetic correction.

The issue of variance and scale in pPCA space is complicated and worth exploring. Tab. 2 summarizes the variance in the traits, evolutionary covariance matrix, eigenvalues, and scores using the same example data from Fig. 2. The total variance in the two traits is the same as reported before, but the sum of the diagonals of the evolutionary covariance matrix $\mathbf{P_P}$ is different because the trait variances have been adjusted to remove the phylogenetic covariances. The eigenvalues are calculated from $\mathbf{P_P}$ so their sum is equal to the trace of $\mathbf{P_P}$ and represents the total amount of variance among the taxa after adjusting for their phylogenetic covariances. In other words, the sum of the eigenvalues is the variance expected if the taxa had been drawn from a star phylogeny.

Importantly, the sum of the variance of the pPCA scores is identical to the sum of the variance of the traits, and to the sum of the variances of ordinary PCA scores (Tab. 2). The variance is conserved in pPCA scores because the tips are rigidly rotated into the pPCA space without consideration of the phylogenetically corrected variance. In other words, the orientation of pPCA axes has been adjusted for the effects of phylogeny, but the spacing of the taxa has not. The conservation of variance in the scores has several effects. First, the distances between tips are identical in the original trait space, PCA space, and pPCA space. We already reported that the average distance between tips in the first two of these spaces was 0.730, and so is their average distance in pPCA space. pPCA thus preserves the distance between objects and their proportionality in exactly the same way that PCA does, meaning that many kinds of analysis, such as morphological disparity, will be unaffected by the choice of ordination technique (see examples below).

Equally importantly, the sum of the variance of the pPCA scores is not the same as the sum of the eigenvalues (Tab. 2). The direction of the ordination of the tips has been adjusted for phylogenetic covariance, but their variance and distances have not. Thus, the distances between tips in the pPCA ordination is just as much affected by phylogeny as in PCA. For this reason, Revell (2009) cautioned that phylogenetic statistics should be used to analyze pPCA scores in cases where one wants to remove the effects of phylogenetic covariance.

pPCA scores are correlated

Even though pPCA axes are orthogonal with respect to each other, pPCA scores are, in fact, highly correlated between axes. In our example (Fig. 2), the scores on PC 1 and PC 2 are uncorrelated (R = 0.0), but the scores on pPC 1 and pPC 2 have a substantial correlation (R = 0.39). The eigenvectors extracted from $\mathbf{P_P}$ are orthogonal, but the scores of the tips are not, which makes them very different from normal PCA shape variables. This fact is an important consideration for further analyses where statistical independence between variables may be required.

Humerus morphology in mammalian carnivores: a worked example

Here, we provide a worked example of a phylogenetic PCA using a humeral dataset from musteloid carnivorans (red pandas, skunks, raccoons, weasels, badgers, otters, and allies) assembled by one of us (A.-C. F.). This sample of small to medium-sized carnivorans is ideal for demonstrating the utility of pPCA, as it includes terrestrial, fossorial, arboreal, and aquatic species, and thus represents considerable ecological and morphological diversity. The humerus is well known to reflect locomotory ecology, and provides a simple example of the relationship between shape, ecology, and phylogeny. However, morphometric analyses of single elements are not without complications. In particular, landmark-based geometric morphometric approaches may be insufficient for analysing structures without points of clear homology, such as articular surfaces of long bones. In order to more accurately represent the morphology of the humerus in the musteloid sample, we gathered landmarks across the humerus, as well as semi-landmarks from the distal articular surface, as described below. This study thus provides an example of pPCA with a highly multivariate dataset that is becoming increasingly common with the growing availability of advanced biological imaging tools.

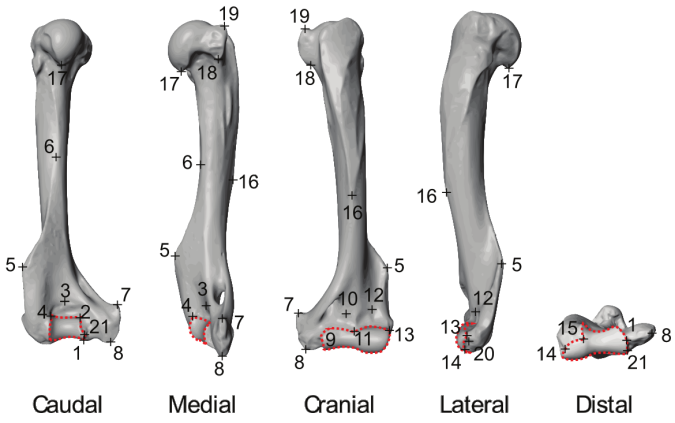

Figure 4 – Three-dimensional landmarks and semilandmarks of the humerus used in the example study. Landmarks are numbered and semilandmarks were placed on the surface outlined in red.

Specimens

Humeri for 29 species of musteloids, spanning their extant diversity, were obtained from the following two collections: the Muséum national d'Histoire naturelle, Paris (*Ailurus fulgens*, *Bassaricyon gabii*, *Bassariscus astutus*, *Conepatus chinga*, *Eira barbara*, *Enhydra lutris*, *Galictis vittata*, *Gulo gulo*, *Lontra felina*, *Lutra lutra*, *Lyncodon patagonicus*, *Martes foina*, *Martes martes*, *Meles meles*, *Mellivora capensis*, *Mustela eversmanii*, *Mustela lutreola*, *Mustela putorius*, *Nasua narica*, *Nasua nasua*, *Neovison vison*, *Poecilogale albinucha*, *Potos flavus*, *Procyon cancrivorus*, *Procyon lotor* and *Pteronura brasiliensis*) and the Naturhistorisches Museum, Basel (*Mydaus javanensis*, *Taxidea taxus* and *Vormela peregusna*). All specimens were adults and predominantly wild caught. Because gender information is often missing from museum specimens, specimens include both male and females. For the purposes of this worked example, only one specimen per species was used in the analyses. In order to perform pPCA on this sample, we used the relevant subset of the supertree of Nyakatura and Bininda-Edmonds (2012). While phylogenetic relationships based on supertree methods are not always congruent with the relationships that would be obtained directly from a combined phylogenetic dataset (Kluge, 1989), this supertree is broadly congruent with carnivoran relationships as they are currently understood.

Shape Coordinates

3-D surface scans of humeri were acquired with a white light fringe Breuckmann scanner (StereoSCAN) using its dedicated scanning software Optocat 2009 (http://www.breuckmann.com). Twenty-one true landmarks and 285 semi-landmarks were selected to represent humeral morphology (Fig. 4, Appendix). The landmarks were gathered using the software package Idav Landmark (Wiley et al., 2005). To generate semi-landmarks a template was created as a reference following the method of Souter et al. (2010). The 3-D sliding landmark procedure (Bookstein, 1997b; Gunz et al., 2005) was used in order to generate landmarks within the boundaries of the template by transforming sliding semi-landmarks into landmarks using Edgewarp3D 3.31 (Bookstein and Green, 2002). The semi-landmarks of the template are warped onto each new specimen within the predefined curves of the template (denoted by the red dotted line in Fig. 4) followed by spline relaxation. Both sliding and relaxation are repeated iteratively until the bending energy is minimized. After this operation has been performed, the landmarks and semi-landmarks are treated identically as variables in the equations described above.

Results

We performed several analyses on both PCA and pPCA scores to demonstrate when the choice of method makes a difference. We looked at the ordinations themselves, plus from the scores we constructed distance-based and trait-based trees, two measures of morphological disparity, and a multivariate regression to find the relationship between shape and a continuous variable, and from the eigenvalues we calculated a simple measure of modularity.

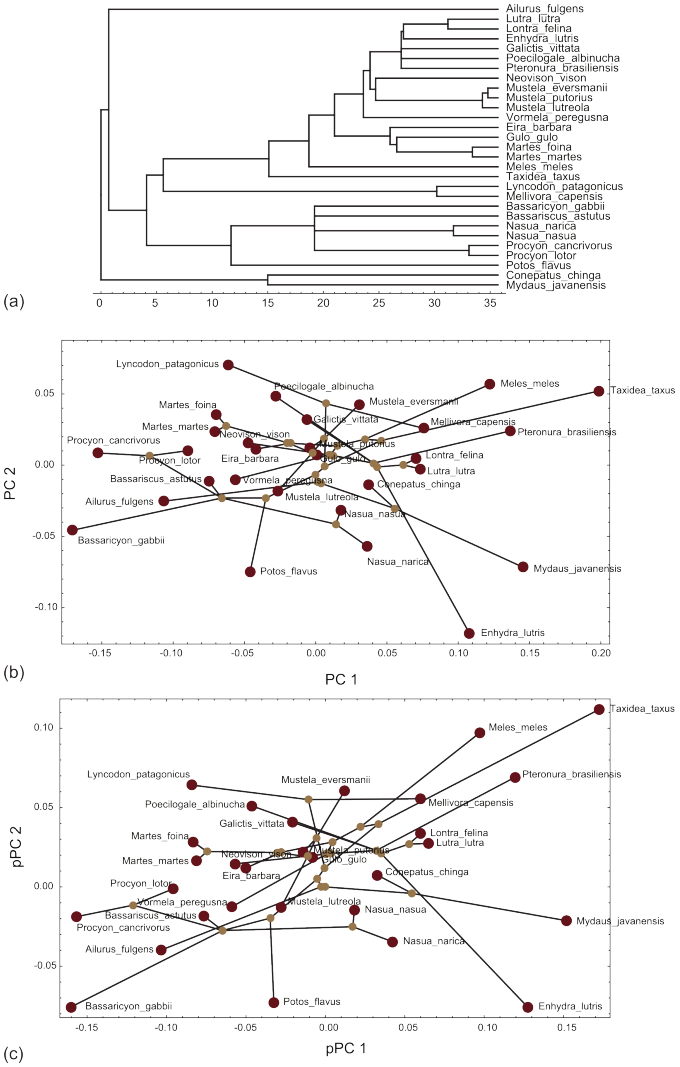

Figure 5 – (a) Phylogenetic supertree of the 29 carnivoran species used in the example data set, taken from Nyakatura and Bininda-Edmonds (2012). (b) PCA ordination of these species based on 21 landmarks and 285 semilandmarks. The phylogenetic supertree for these species has been projected into the space. (c) Phylogenetic PCA of the same data. The first two axes of these ordinations are different, but due to the considerable homoplasy in humeral shape among these taxa the two ordinations are very similar. Note that there are 26 additional dimensions to the shape space other than those shown here.

The PCA and pPCA ordinations were similar but not identical, even though the phylogenetic tree used to produce the pPCA axes has a lot of structure (Fig. 5). The fact that the two ordinations are rigid rotations (plus translation) of each other can be seen in the plots, even though only the first two dimensions of the shape spaces are visible. Inspection of the plots reveals that humeral shape has considerable homoplasy, with lineages from different clades independently colonizing some regions of shape space. The homoplasy in this data set is probably responsible for the strong similarity in the two ordinations, having masked most of the phylogenetic covariance in shape.

Distance-based trees based on the two sets of scores were identical (Fig. 6a-b). These are UPGMA trees constructed from Euclidean distance matrices of the scores of the PCA and pPCA ordinations. Because inter-object distances are preserved in both kinds of ordination, the distance matrices are identical; hence the trees are, too.

Trait-based trees were marginally different for PCA and pPCA (Fig. 6c-d). The trees shown here are maximum-likelihood trees using the continuous traits algorithm implemented in PHYLIP (Felsenstein, 1973, 2009). This algorithm treats each trait, which consists of scores on the 28 principal component axes, as independent in estimating the

tree. The PCA and pPCA trees are different because the axes differ between the analyses, and because the pPCA scores are not actually independent (uncorrelated) meaning that some of them contain redundant information that causes some aspects of shape variation to be overweighted in the estimation of the ML tree.

Table 3 – Comparison of results of follow-up analyses performed using PCA and pPCA scores as shape variables.

Analysis	PCA scores	pPCA scores
UPGMA tree	Identical	
ML tree	Different	
Disparity (Mean pairwise Procrustes distance)	0.174	0.174
Disparity (Mean Procrustes distance to mean)	0.121	0.121
R^2 of shape on centroid size	0.03	0.03
Eigenvalue variance	0.964	0.965
Eigenvalue standard deviation	0.00029	0.00003

Measures of disparity were identical between PCA and pPCA (Tab. 3). Since disparity is a measure of morphospace occupation, it is based on any one of several measures of between-specimen distances (Foote and Miller, 2007). We calculated two disparity metrics, the mean multivariate inter-species distance (which in this case is the Procrustes distance between species) and the mean multivariate distance (Procrustes distance) between species and their group mean. When all dimensions of the shape space are used, these disparity metrics are identical between PCA and pPCA because distances between objects are preserved in both these analyses. If only the first two axes were used to calculate disparity, the results would be different (but the results would not be based on actual differences in shape, only on an arbitrarily defined subcomponents of shape difference).

The proportion of variance explained by multivariate regression of shape onto log centroid size (R^2) was also identical between PCA and pPCA (Tab. 3). The regression coefficients of each individual PC differed slightly (not shown), because the PCs each represent a different component of variance in the two analyses, but the overall relationship between shape and size is conserved because the shape variables collectively describe the same shape variation in PCA and pPCA, thus the proportion of shape variance explained is identical.

Measures of eigenvalue dispersion, a straightforward and commonly used estimate of morphological integration (Pavlicev at al., 2009; Goswami and Polly, 2010) were also compared between PCA and pPCA. While eigenvalue variance was nearly identical in the two analyses (Tab. 3), eigenvalue standard deviation, which may be a more reliable indicator of integration, was tenfold higher in PCA than in pPCA. In part the difference is due to the arbitrary scaling of the covariances introduced by the branch length units in Equation 4 of pPCA, but the difference is also due to non-proportional changes in the estimated covariance structure from having removed the phylogenetic covariances. Thus eigenvalue dispersion measured from pPCA eigenvalues suggests lower integration in the musteloid humerus than does the dispersion of eigenvalues from PCA. Some of the integration in the ordinary PCA results arises from the phylogenetic covariance of the taxa.

Discussion

Phylogenetic PCA is a compromise between non-phylogenetic variance and total shape variance

The axes in pPCA describe the non-phylogenetic component of shape covariance and, as a result, they are independent from phylogeny and orthogonal to one another (Revell, 2009). On average, the eigensystem derived from the phylogenetically corrected covariance matrix is more closely related to the generating covariances than the uncorrected matrix (Revell, 2009). In some cases, such as our simulated example, the uncorrected matrix and the first PC are also highly correlated with the generating covariances, but this will depend on tree balance and mode of evolution. The scores of objects projected onto pPCA axes are neither independent of phylogeny nor orthogonal with respect to each other, however (as clearly stated by Revell 2009). The scores are obtained by rigid rotation of the original data to the pPCA eigenvectors, which preserves the inter-object shape distances, but also preserves the phylogenetic structure in the data. The only difference between a pPCA ordination and regular PCA is that the axes are oriented differently and centered on a different point. The trajectory of shape variation along the pPC 1 is by definition a trajectory parallel to the major non-phylogenetic axis of variation, but the spacing of objects along pPC 1 includes phylogenetic similarity and difference. The visual information conveyed by the spacing of objects in a pPCA plot thus contains a significant phylogenetic component.

Non-independence of scores on pPCA axes may affect some kinds of analysis but not others

Scores of objects on pPCA axes are correlated, whereas PCA scores are uncorrelated across axes. Statistical independence is a desirable property in shape coordinates that are used for tree building, statistical analysis, or shape modeling (Rohlf, 1993), but it is not a requirement if the subsequent analysis does not assume independence of its input variables. All of the analyses we applied to the example data set were based on algorithms that take into account non-independence except for maximum-likelihood tree building for continuous traits. Consequently, results from PCA and pPCA were identical except for the ML tree. pPCA scores can, therefore, be safely used as shape variables for most applications, just as partial warps scores (Bookstein, 1997a) can be used as shape variables even though they are similarly co-dependent (Zelditch et al., 2004).

Dimensionality of pPCA space is appropriate for shape analysis

Removal of the phylogenetic component of shape variance in the calculation of pPCA space does not change its dimensionality. The number of pPC axes with non-zero variance is the same as the number of ordinary PC axes, and that number is $2k-4$ for two-dimensional landmarks and $3k-7$ for three-dimensional landmarks (Rohlf and Slice, 1990; Rohlf, 1999). pPCA scores thus have appropriate dimensionality for further statistical analysis.

Adaptation versus direct environmental effects: Phylogenetic correction can be the wrong approach

Phylogenetic comparative methods are often employed for studying the relationship between phenotypes and environment, but not all environmental effects on morphology arise from non-phylogenetic sources. When the phylogenetic changes are adaptive (*sensu* Gould and Vrba 1982), then environmental components of variation are identical to phylogenetic components. Greene (1986) and Coddington (1988) provided a rigorous phylogeny-based method for studying adaptation, arguing that for a phenotypic change to be considered adaptive, it must have arisen on a phylogenetic tree at the same point as its associated change in function. In other words, functional (or environmental) change must be perfectly correlated with phylogeny. Removing phylogenetic correlations from data will remove precisely the component of shape variation that is relevant to adaptation.

Too often phylogenetic comparative methods are used to remove the effects of phylogeny when the processes being studied are, in fact, phylogenetic rather than non-phylogenetic (Westoby et al., 1995). Conflation of non-phylogenetic and environmental components of variation in the literature probably arises by false analogy with the quantitative genetics concepts of "genetic" and "environmental" components of phenotypic variance (Falconer and Mackay, 1996; Lynch and Walsh, 1998). Phylogenetic comparative methods similarly partition phenotypic variance among taxa into phylogenetic and non-phylogenetic components (Martins and Hansen, 1997; Felsenstein, 2003), but the analogy that the non-phylogenetic component is "environmental" and the phylogenetic component is not does not hold. Rather, the non-phylogenetic component of comparative data is the component associated with universal factors that affect organisms regardless of their

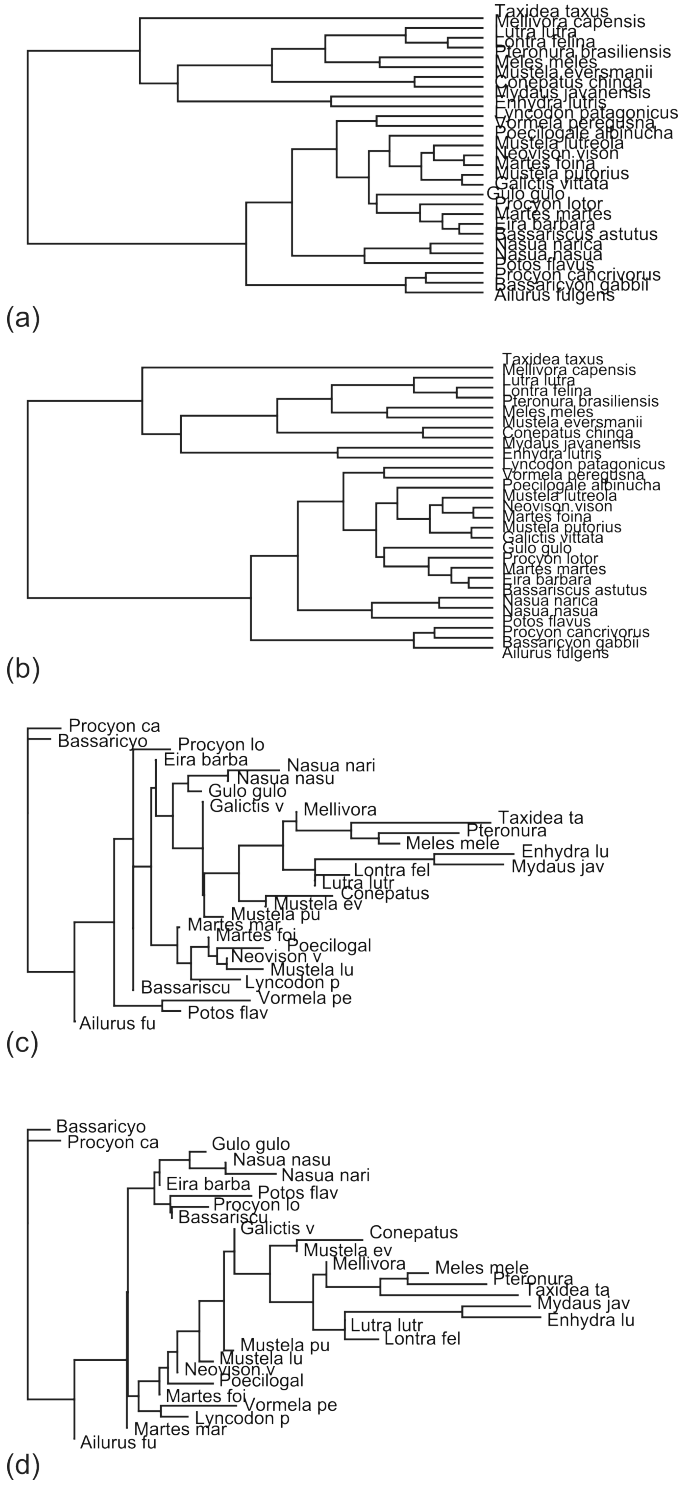

Figure 6 – Trees constructed from PCA and pPCA scores. UPGMA trees constructed from PCA scores (a) and pPCA scores (b). These trees are based on inter-object distances, which are conserved by these two methods, and so they are identical. Continuous-trait maximum-likelihood trees constructed from PCA scores (c) and pPCA scores (d). The ML method treats each PC as if it were an independent trait. Because PCA and pPCA find different axes and because pPCA scores are intercorrelated, the two ML trees are different (though only minorly so for this particular data set).

phylogenetic relationship, whereas the phylogenetic component of variation is the component shared through ancestry. pPCA may therefore not be appropriate if adaptation of morphology is being studied, or if homoplasy is being assessed.

Similarly, the removal of phylogenetic covariances in analyses of modularity or morphological integration should be carefully considered. In the musteloid humerus example, measures of eigenvalue dispersion were very similar for PCA and pPCA, but eigenvalues from pPCA did show lower standard deviation, and thus lower integration, than those from PCA. A strong relationship between generating covariances, such as those driven by genetic and development effects, and phylogenetic covariances may be expected, as evolution along any branch will be strongly influenced by the generating covariances. Moreover the genetic and developmental drivers of morphological integration and modularity inevitably correlate strongly with phylogeny. Removing the phylogenetic covariances may thus also obscure the real modularity or integration of a structure. For some analyses of modularity, it may be appropriate to remove phylogenetic effects prior to analysis of trait covariances, but, as with environmental effects, using phylogenetic comparative has the capacity to obscure, as well as to reveal, evolutionary relationships among traits.

Conclusions

Phylogenetic PCA belongs to the class of phylogenetic comparative methods that remove the expected covariance among objects prior to statistical analysis. The general purpose of such methods is to correct the statistical non-independence of data points that arises from shared phylogenetic history for tests whose p-values depend on the assumption that data points are independent (e.g., the probability that the slope of a regression line significantly differs from zero). These methods down-weight the contribution of closely related taxa to test the relationship between phenotype and associated function or environment because each of close relatives is putatively sampling the same evolutionary adaptation in their common ancestor. Phylogenetic PCA is an unusual example of phylogenetic comparative methods because it is not an analysis *per se* and it serves as a replacement for ordinary PCA, even though the latter does not depend in any way on objects being statistically independent. pPCA is a potentially confusing mixture of major axes that describe non-phylogenetic variation and scores that contain phylogenetic components of variation. The individual axes of pPCA therefore are not usually aligned with clade differences; however, phylogenetic groupings are still equally as evident in pPCA as they would be in ordinary PCA. Potentially undesirable properties of pPCA are that the scores are correlated between axes, the variance of scores on pPC axes does not necessarily decrease with sequentially higher axes, and pPCA scores are not phylogenetically corrected for purposes of subsequent analysis. Nevertheless, pPCA space can be used for geometric morphometric shape modeling and its scores have other properties that are desirable for shape variables, such as having the correct dimensionality and being complete descriptors of shape variation. Phylogenetic principal components analysis can, therefore, be included among the tools available for geometric morphometric analysis as long as it is used knowledgably.

References

Ackerly D.D., Donoghue M.J., 1998. Leaf size, sapling allometery, and Corner's rules: phylogeny and correlated evolution in maples (*Acer*). Am. Nat. 152: 767–791.

Adams D.C., Collyer M.L., 2009. A general framework for the analysis of phenotypic trajectories in evolutionary studies. Evolution 63: 1143–1154.

Bergmann P.J., Berk C.P., 2012. The evolution of positive allometry of weaponry in horned lizards (*Phrynosoma*). Evol. Biol. 39: 311–323.

Bookstein F.L., 1997a. Morphometric Tools for Landmark Data: Geometry and Biology. Cambridge University Press: Cambridge, UK.

Bookstein F.L., 1997b. Landmark methods for forms without landmarks: morphometrics of group differences in outline shape. Med. Image Anal. 3: 225–243.

Bookstein F.L., Green W.D.K., 2002. Users Manual, EWSH3.19. Available at http://brainmap.stat.washington.edu/edgewarp/

Coddington J.A., 1988. Cladistic tests of adaptational hypotheses. Cladistics 4: 3–22.

Dryden I.L., Mardia K.V., 1998. Statistical Shape Analysis. Wiley: Chichester, UK.

Falconer D.S., Mackay T.F.C., 1996. Quantitative Genetics. Benjamin Cummings: San Francisco, California.

Felsenstein J., 1973. Maximum-likelihood estimation of evolutionary trees from continuous characters. Am. J. Human Genet. 25: 471–492.

Felsenstein J., 2003. Inferring Phylogenies. Sinauer Associates: Sunderland, Massachusetts.

Felsenstein J., 2009. PHYLIP (Phylogeny Inference Package) version 3.6.9. Distributed by the author. Department of Genome Sciences, University of Washington: Seattle.

Foote M., Miller A.I., 2007. Principles of Paleontology. W.H. Freeman: New York.

Goswami A., Polly P.D., 2010. Methods for studying morphological integration, modularity and covariance evolution. In: Alroy J., Hunt G. (Eds.). Quantitative Methods in Paleobiology. Paleontological Society Short Course. The Paleontological Society Papers 16: 213–243.

Gould S.J., Vrba E.S., 1982. Expatation – a missing term in the science of form. Paleobiology 8: 4–15.

Greene H.W., 1986. Diet and arboreality in the Emerald Monitor, *Varanus prasinus*, with comments on the study of adaptation. Fieldiana Zool. 31: 1–12.
Gunz P., Mitteroecker P., Bookstein F.L., 2005. Semi-landmarks in three dimensions. In: Slice D. (Ed.). Modern Morphometrics in Physical Anthropology. Kluwer Academic/Plenum Publishers: New York.
Jollife I.T., 2002. Principal Components Analysis, 2nd Edition. Springer: New York.
Klingenberg C.P., Gidaszewski N.A., 2010. Testing and quantifying phylogenetic signals and homoplasy in morphometric data. Syste. Biol. 59: 245–261.
Kluge A.G., 1989. A concern for evidence and a phylogenetic hypothesis of relationships among *Epicrates* (Boidae, Serpentes). Syst. Zool. 38: 7–25.
Kohlsdorf T., Navas C., 2012. Evolution of form and function: morphophysiological relationships and locomotor performance in tropidurine lizards. J. Zool. 288: 41–49.
Lynch M., Walsh B., 1998. Genetics and the analysis of quantitative traits. Sinauer Associates: Sunderland, Massachusetts.
Maddison W.P., 1991. Squared-change parsimony reconstructions of ancestral states for continuous-valued characters on a phylogenetic tree. Syst. Biol. 40: 304–314.
Martins E.P., Hansen T.F., 1997. Phylogenies and the comparative method: a general approach to incorporating phylogenetic information into the analysis of interspecific data. Am. Nat. 149: 646–667.
Mitteroecker P., Gunz P., Bernhard M., Schaefer K., Bookstein F.L., 2004. Comparison of cranial ontogenetic trajectories among great apes and humans. J. Human Evol. 46: 679–698.
Nyakatura K., Bininda-Edmonds O.R.P., 2012. Updating the evolutionary history of Carnivora (Mammalia): a new species-level supertree complete with divergence time estimates. BMC Biology 10: 12.
Pavlicev M., Cheverud J.M., Wagner G.P., 2009. Measuring morphological integration using eigenvalue variance. Evol. Biol. 36: 157–170.
Polly P.D., 2004. On the simulation of the evolution of morphological shape: multivariate shape under selection and drift. Palaeontol. Electronica 7.2.7A: 1–28.
Polly P.D., 2008. Adaptive Zones and the Pinniped Ankle: A 3D Quantitative Analysis of Carnivoran Tarsal Evolution. In: Sargis E., Dagosto M. (Eds.). Mammalian Evolutionary Morphology: A Tribute to Frederick S. Szalay. Springer, Dordrecht: The Netherlands. 165–194.
Polly P.D., 2012a. Geometric morphometrics for Mathematica. Version 9.0. Department of Geological Sciences, Indiana University, Bloomington, Indiana. Available from: http://mypage.iu.edu/~pdpolly/Software.html.
Polly P.D., 2012b. Phylogenetics for Mathematica. Version 2.1. Department of Geological Sciences, Indiana University, Bloomington, Indiana. Available from: http://mypage.iu.edu/~pdpolly/Software.html.
Revell L.J., 2009. Size-correction and principal components for interspecific comparative studies. Evolution 63: 3258–3268.
Rohlf F.J., 1993. Relative warp analysis and an example of its application to mosquito wings. In: Marcus L.F, Bello E., Garcia Valdecasas A. (Eds.). Contributions to Morphometrics. Museo National de Ciencias Naturales, Madrid. 131–159.
Rohlf F.J., 1998. On applications of geometric morphometrics to studies of ontogeny and phylogeny. Syst. Biol. 47: 147–158.
Rohlf F.J., 1999. Shape statistics: Procrustes superimpositions and tangent spaces. J. Classif. 16: 197–223.
Rohlf F.J., 2001. Comparative methods for the analysis of continuous variables: geometric interpretations. Evolution 55: 2143–2160.
Rohlf F.J., 2002. Geometric morphometrics and phylogeny. In: MacLeod N., Forey P.L. (Eds.). Morphology, Shape, and Phylogeny. Taylor and Francis: London. 175–193.
Rohlf F.J., 2003. Bias and error in estimates of mean shape in geometric morphometrics. J. Human Evol. 44: 665–683.
Rohlf F.J., Slice D., 1990. Extensions of the Procrustes method for the optimal superimposition of landmarks. Syst. Zool. 39: 40–59.
Schluter D., Price T., Mooers A.Ø., Ludwig D., 1997. Likelihood of ancestor states in adaptive radiation. Evolution 51: 1699–1711.
Souter T., Cornette R., Pedraza J., Hutchinson J.R, Baylac M., 2010. Two applications of 3D semi-landmark morphometrics implying different template designs: the theropod pelvis and the shrew skull. C. R. Palevol 9: 411–422.
Westoby M., Leishman M.R., Lord J.M., 1995. On misinterpreting the "phylogenetic correction". J. Ecol. 83: 531–534.
Wiley D.F., Amenta N., Alcantara D.A., Ghosh D., Kil Y.J., Delson E., Harcourt-Smith W., Rohlf F.J., St John K., Hamann B., 2005. Evolutionary morphing. In: Proceedings of IEEE Visualization 2005 (VIS'05), 23-28 October 2005, Minneapolis, MN, USA.
Zelditch M.L., Swiderski D.L., Sheets H.D., Fink W.L., 2004. Geometric Morphometrics for Biologists: A Primer. Elsevier Academic Press: San Diego, California.

Associate Editor: A. Cardini

Appendix

Definitions of the 21 landmarks used in the example study of carnivoran humerus shape.

Landmark	Definition
1	Most medio-distal point of the caudal part of the capitulum
2	Most medio-proximal point of the caudal side of the capitulum
3	Point of maximum of curvature of the olecranon fossa
4	Most latero-proximal point of the caudal side of the capitulum
5	Point of maximum of convexity of the lateral epicondylar ridge
6	Point of insertion of the lateral epicondylar ridge on the diaphysis
7	Most proximal tip of the entepicondylar area
8	Most distal tip of the entepicondylar area
9	Most medio-proximal point of the cranial side of the capitulum
10	Point of maximum of curvature of the coronoid fossa
11	Most proximal point of contact between the trochlea and the capitulum
12	Point of maximum of curvature of the radial fossa
13	Most latero-proximal point of the cranial side of the capitulum
14	Most disto-lateral point of the capitulum
15	Most distal point of contact between the trochlea and the capitulum
16	Most distal point of the deltopectoral crest
17	Tip of the lesser tuberosity
18	Most proximo-medial point of the greater tuberosity
19	Most disto-medial point of the greater tuberosity
20	Most latero-distal point of the cranial side of the capitulum
21	Point of maximum of concavity of the caudo-medio-distal part of the capitulum